ADVANCES IN PHYSICS: X
2020, VOL. 6, NO. 1, 1843535
https://doi.org/10.1080/23746149.2020.1843535

Taylor & Francis
Taylor & Francis Group

REVIEW

Optical vortex knots and links via holographic metasurfaces

Peng Li[a], Xuyue Guo[a], Jinzhan Zhong[a], Sheng Liu[a], Yi Zhang[b], Bingyan Wei[a] and Jianlin Zhao[a]

[a]MOE Key Laboratory of Material Physics and Chemistry under Extraordinary Conditions, and Shaanxi Key Laboratory of Optical Information Technology, School of Physical Science and Technology, Northwestern Polytechnical University, Xi'an, China; [b]School of Chemical and Biomedical Engineering, Nanyang Technological University, Singapore, Singapore

ABSTRACT

Vortices arise in many natural phenomena as dark points of total destructive interference. Sometimes they form continuous lines and even enclosed loops with knotted or linked topologies in three spatial dimensions. Since the mathematical topology was introduced into physics, from hydrodynamics, condensed matter physics to photonics, and other modern physical fields, scientists have been exploring the related topological essences of vortex knots; hence, the topology is a forefront topic in different physical systems. Owing to the reliability and observability of light in free space, optical vortex knots and links are the most studied physical topologies. Here, we review some of these developments with a focus on optical vortex knots and links. We first introduce the brief historical perspective and structural properties of optical vortices. Then, we trace the progress on the theoretically constructing, experimentally generating, and characterizing methods of topological light fields. Wherein, we review recent developments of holographic metasurfaces and their applications in generating ultrasmall optical vortex knots. At last, we envision the possible challenges and prospects of topological light fields.

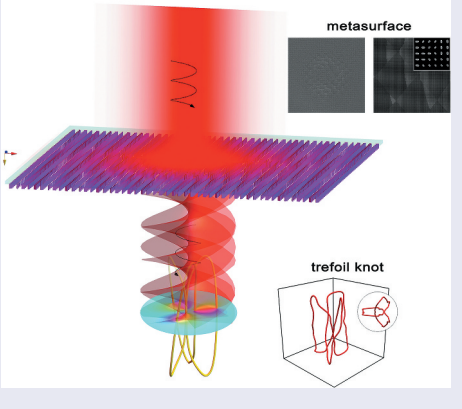

ARTICLE HISTORY
Received 31 August 2020
Accepted 24 October 2020

KEYWORDS
Optical vortex; knot; topology; metasurface; holography

CONTACT Jianlin Zhao jlzhao@nwpu.edu.cn; pengli@nwpu.edu.cn MOE Key Laboratory of Material Physics and Chemistry under Extraordinary Conditions, and Shaanxi Key Laboratory of Optical Information Technology, School of Physical Science and Technology, Northwestern Polytechnical University, Xi'an 710129, China

1. Introduction

Vortices as phase singularities are a common phenomenon in nature, ranging from water and atmosphere circulation to condensed state in electronic systems, and even spiral galaxies [1–3]. In a complex scalar wavefield, vortex singularities are as locations where phases are undefined, and the intensities of the field are zero. They were first postulated by Whewell in the 1830s based on the observation of ocean wave [4], which may be considered as a complex scalar field, that amphidromic points exist in the tides, as the crosses of tides. Beyond the wave phase, in quantum physics, vortices represent quantized flux circulations of some physical quantities as topological defects, determining the properties of quantized systems [5–9]. The nontrivial dynamics of vortices in classical and quantum systems have evoked extensive interests [10–15] and brought significant opportunities for the exploration of new wave transmission and the realization of accurate wavefield manipulation, such as directional energy transport [16], topological quantum computation [17], topological information [18] and so on.

The serious study of vortices began in 1974, when Nye and Berry studied the position-dependent amplitude of ultrasound reflected from the ice covering Antarctica [19]. In the recorded intensity and phase distribution of scattered ultrasound reflected from the experimental model, they observed intensity nulls surrounded with changed phase from 0 to 2π and defined such special singularities as 'wave dislocation', analogous to the planes of atoms around dislocations in crystals. In 1989, Coullet firstly used the term 'optical vortex' to describe a possible laser mode having phase singularity [20]. Subsequently, as the recognition of orbital angular momentum (OAM) [21], which manifests itself as an intrinsic property of photon, optical vortices have been intensively studied due to their enormous application potentials [22–26].

Simultaneously, particular interests were traced into three-dimensional (3D) structures of vortex. Since the topology (in mathematics, topology describes the nature of geometric figures or spaces that can remain unchanged after continuously changing shapes) was introduced into the physical domain, various topological configurations, and associated dynamics in disparate fields have been discovered [27–35], boosting the emergence of a large number of striking wavefields, and novel topological materials such as topological insulators, topological semimetals, and topological superconductors [36–38]. Novel physical phenomena related to topological states are also radiated from condensed electronic systems to fluid, phonons, and other systems [39–42].

In light field, optical vortices form curved lines, namely, nodal lines, and tangle three-dimensionally to configure topological structures, such as knots

and links [3]. Such intriguing spatially structured light fields with phase singularities in real space, exhibit broad application prospects in optical manipulation, optical communication, and quantum information transmission [26,43,44]. Moreover, topology can be considered as the exploration of itself, i.e. 3D structural properties, as a new degree of freedom in photonics that is different from the traditional modulation parameters such as amplitude, phase, and polarization [45]. Knotted and linked light fields, as a new family of null solutions to Helmholtz equation in 3D free space, have attracted increasing interests because of their prominent spatial feature and the unique opportunity that combines the experimental and analytical studies of common topological properties in disparate matter systems [45–48].

Here, we report on the recent progress of 3D vortex, more specifically, optical vortex knots and links. The contents are organized as follows. Firstly, we begin with a brief historical perspective and structural features of vortex knots and links. Then we trace the progress on the generating and characterizing methods referring to topological light fields. We discuss recent developments in holographic metasurfaces: high efficiency, multi-parameter and wideband response, and their applications in generating ultrasmall optical vortex knots. At last, we give an overview on the outlook of anticipated future expansion of the topological light fields.

2. Optical vortex

The study of optical vortices can be dated back to the research of Goos–Hänchen shift, that Wolter discovered wave circulation induced by a street of vortices with alternating signs, which was in the phase pattern of interference field composed by the incident and reflected plane waves, as well as evanescent waves [3]. Subsequently, this circulation phenomenon associated with optical vortex was demonstrated to be quite general in light fields as the result of multiple wave interference. For instance, Braunbek recognized that three plane waves were sufficient to produce energy vortices, and found vortices in Sommerfeld's exact solution of a plane wave diffracted by an infinite halfplane. Meanwhile, the exploitation of beams bearing phase singularities was also underway. Remarkably, Vaughan and Willettes investigated the properties of light beams with phase singularities and their interference along the beam axis [49].

Optical vortices, as a ubiquitous phenomenon in interference, naturally occur in the superposition field [3,50]. In three spatial dimensions, phase singularities continuously distribute in the form of tangled vortex lines, that is, threads of darkness in light fields [51]. Take a random speckle as an example, which is the interference pattern generated by the random scattering of a coherent source and can be described as the superposition of a large

number of random plane waves with different wavevectors, in which these 3D configurations of the vortex line are mainly divided into the following two categories [52].

The first type, passing through the entire volume as unbounded line, as the red lines shown in Figure 1(a), which exists typically in the superposition field of three plane waves with different wave vectors [3]. Since such kind of vortex lines extends on axis, or parallel to the axis, the topologies are structurally stable during beam propagating. Therefore, researches are mostly focused on the transverse modes with helical phase patterns and the associated energy flow distributions of light beams [53]. In this case, the vortex is characterized by a topological index, namely, topological charge, which depicts the change of phase φ along a circuit C enclosing the phase singularity in the lateral plane, quantized in units of 2π:

111(1)

where l is the so-called topological charge of optical vortex. Inspired by the exploitation of Vaughan and Willets [20], cylindrically symmetric higher-order beams, as transverse eigenmodes of laser cavity, were discovered carrying inherent optical vortices on axis. Thus, the topological charge is an essential parameter to characterize optical vortex and the carrier beam. Laguerre-Gauss (LG) beams and Bessel–Gauss (BG) beams [21,54], the so-called vortex beams, are examples. Figure 2 displays the transverse amplitude and phase patterns, as well as helix wavefronts of the LG (l,p) beams with different topological charges and radial indices (denoted as p), respectively [26].

In the past two decades, the properties of vortex beams have been extensively studied, since the breakthrough made by Allen [21]. He pointed

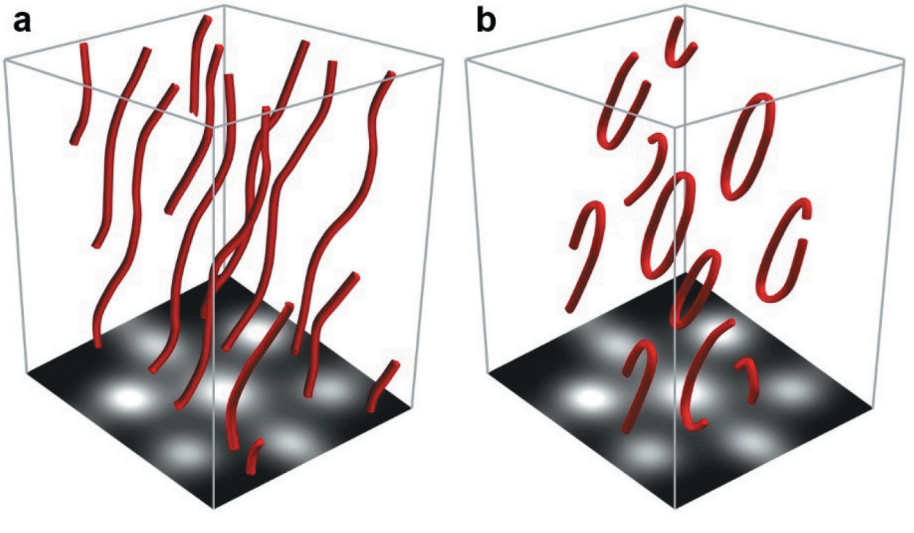

Figure 1. Two kinds of vortex lines in the 3D free space. (a) Infinite vortex lines. (b) Vortex loops.

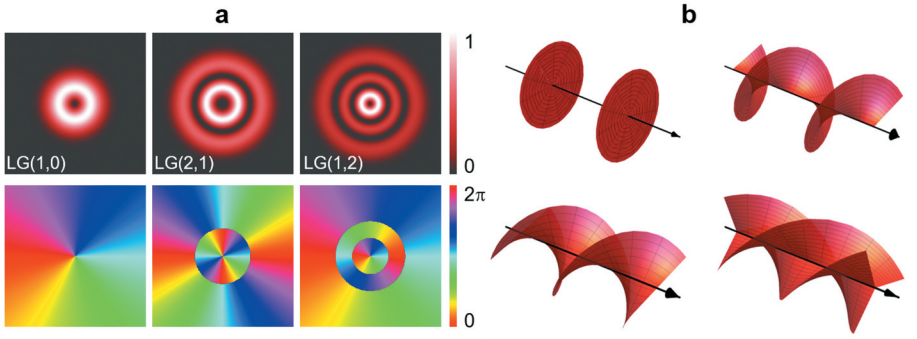

Figure 2. Vortex lines in laguerre-gauss (LG) modes [26]. (a) Transverse intensity (top) and phase (bottom) distributions of the LG(1,0), LG(2,1), and LG(1.2) modes. Those numbers in brackets depict the azimuthal (topological charge *l*) and radial (denoted by *p*) indices, respectively. (b) Helical wavefronts and on-axial vortex lines of LG modes in 3D space. Their topological charges are 0, 1, 2, and 3, respectively.

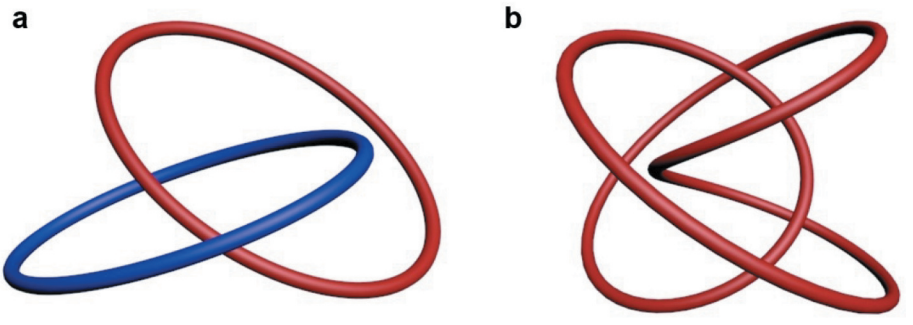

Figure 3. Examples of optical vortex (a) link and (b) knot.

out that the LG beams carry intrinsic OAMs quantified as $l\hbar$ along their axis, analogous to the spin angular momentum $\sigma\hbar$ with $\sigma = \pm 1/2$ denoting the spin quantum number. Due to the transfer possibility of OAM from photons to particles, the vortex beams were often used as optical spanner to manipulate particles [24]. On the other hand, because these photon OAMs can form qubits in high-dimensional Hilbert space, vortex beam can be further used for information transmission [22]. Particular interests have been concentrated on the interaction of angular momenta, i.e. spin-orbit coupling, which produced marvelous evolutions of light fields such as spin Hall effect of light [55–58]. These related performances of optical vortices have been introduced into electric beams, atom beams, and even matter wave systems [59–61].

The other type, which approximates 27% of total vortex lines, connects themself to form closed loops [52], as shown in Figure 1(b), with complex topologies as links or knots, as shown in Figure 3. These configurations occur in the superposition of waves more than three and represent the global topology of light fields [62]. Since the vortex line always occurs on the intersection of the wavefront surfaces with all phase labels, these topologically structured vortex lines indicate that all wavefront surfaces have a knotted boundary curve, and are thus multiply connected. Although the vortex topology occupies a finite volume of space, it affects the entire wavefield. Therefore, such nontrivial topologies of optical vortex widely arising elsewhere in physics, such as flows in fluid dynamics [42], quantum condensates [63], and field theory [34], have received considerable concern.

3. Optical vortex knots and links

Knots are defined mathematically as closed curves in the 3D free space. The first description of vortex knot can be tracked back to the hypothesis of Lord Kelvin that atoms were naturally knotted vortex loops in the ether. Although this hypothesis has been falsified, the remarkable topology theory has

inspired the development in mathematical knot and many physical fields, where knotted vortices have long been thought to play an important role. In recent years, it has become experimentally accessible in disparate physical systems [31,42,48]. Therein, the topological skeleton unites those many seemingly unrelated physical phenomena. The construction of vortex lines and related topology modulation in these systems is an area of intense theoretical and experimental investigation.

As the initial conceive of introducing topology concept, knot has been studied as a fundamental conserved quantity in fluid mechanics for a long time, but this conservation characterization in the presence of dissipation has proven difficult to resolve [42]. Although the topology conservation in conventional fluids is unprocurable, due to the inherent nonlinearity of most dynamic fields, this challenging performance has been achieved in superfluid [64]. In contrast, universality and the stability of linear homogeneous media in optical system have evoked tremendous interests to exploit the optical counterparts.

As originally emphasized by Nye and Berry, optical vortices are naturally curved lines embedded in 3D wavefields [19]. Optical vortex lines are naturally found throughout optical speckle [52], occurring as dark points where the singularity lines intersect the imaged plane. In 3D optical speckle, these vortex lines form fractal tangles, percolating through space with many closed loops that are linked together. However, how to construct stable and isolated vortex knots in a limited space, especially in a propagating light

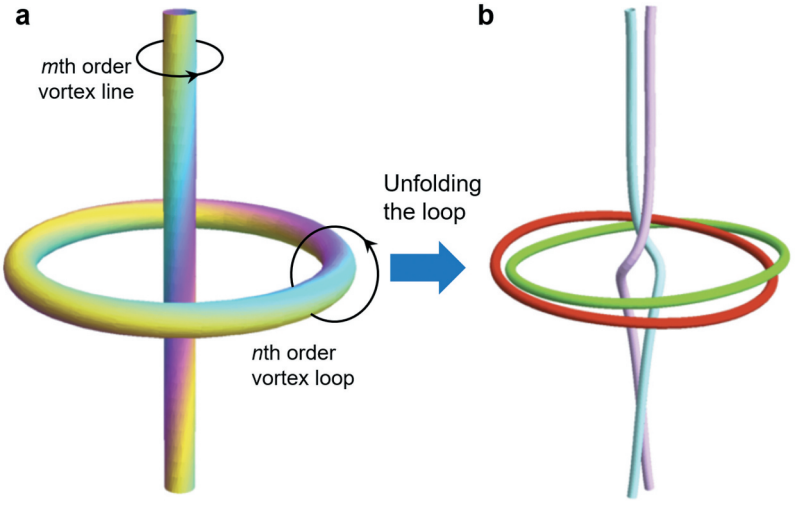

Figure 4. Unfolding operation of perturbation on an unstable high-order vortex loop [51]. (a) An unstable *n*th order vortex loop threaded by a *m*th order axial vortex line. (b) Stable unfolding structure: a ($m = 3$, $n = 2$) torus knot threaded by a triple-stranded helix. Figures reproduced from ref [3]., copyright 2009, Elsevier.

beam, is a prerequisite to reveal the topology property and explore practical applications.

4. Design methods

Tying isolated optical vortex knots and links, the theoretical challenge lies in finding the topologically nontrivial solutions to complex scalar Helmholtz equation in all three dimensions. In 2001, Berry and Dennis first answered this question by theoretically constructing explicit and exact solutions of Helmholtz equation [51], in which the optical vortex lines can be knotted or linked, via the unfolding operation of a perturbation on unstable vortex loops. The wave function of this process can be described as $\Psi(r) = A(r)\exp(il\phi) + \Psi_{\text{perturb}}(r)$, where r and ϕ were the cylindrical coordinates. For the explicit construction, the superposition of Bessel beams, i.e. $A(r)\exp(il\phi)$, which were exact solutions themselves, was chosen to implement a high-order dislocation loop, then a perturbated Gaussian background, i.e. $\Psi_{\text{perturb}}(r)$, was introduced to unfold this single vortex loop into knotted or linked vortex line. Figure 4 schematically shows the unfolding operation [51].

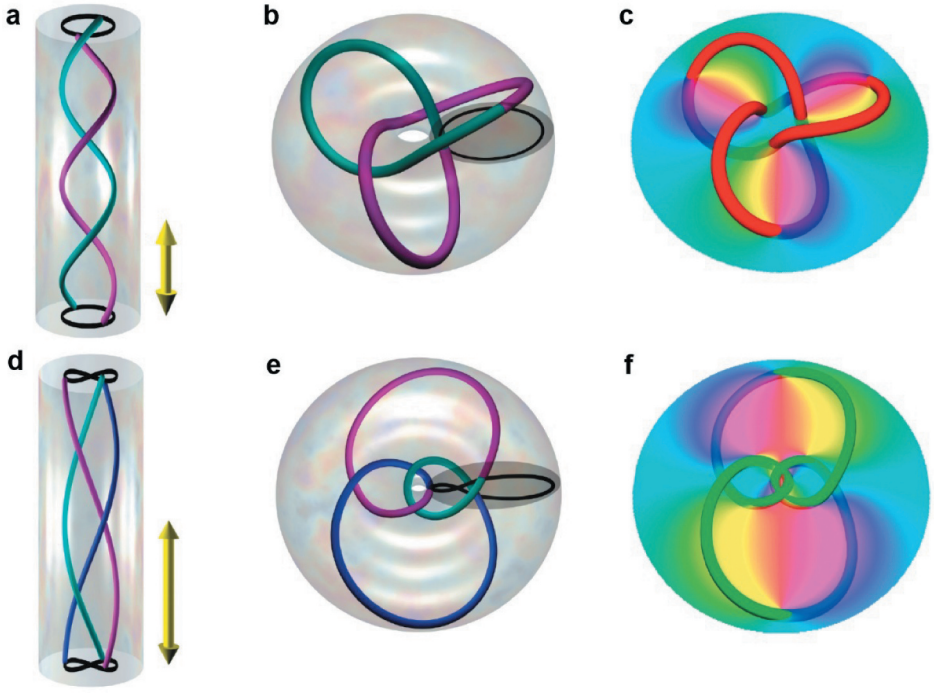

Figure 5. Milnor mapping of braided vortex lines into knots [48]. (a), (d) Braided vortex lines enclosed in a cylinder. (b), (e) Knotted vortex lines lying on the surface of a torus in the 3D space, where vortex lines wind n times around a circle inside the torus and m times around a line through the hole in the torus. (c), (f) Trefoil and Figure-8 knots (lines) and the phases at the $z = 0$ plane. Figures reproduced from ref [48]., copyright 2010, nature publishing group.

Subsequently, the LG set of optical modes that contain on-axial vortex lines with different waist widths, as a convenient basis for specifying modal superpositions, was utilized by Leach to experimentally realize the same topological configuration [31]. The other vortex topologies have also been generated in a specific superposition of beams, e.g. linked and knotted synthetic magnetic fields [65].

As shown in Figure 4(b), these previous vortex knots and links must be threaded by infinite vortex lines, which destroy the topology configuration as a single unit and underlying wavefront topology of interest. To construct isolated vortex knots and links, the Milnor map that describes complex scalar fields with knotted zero lines, as polynomial expansions around

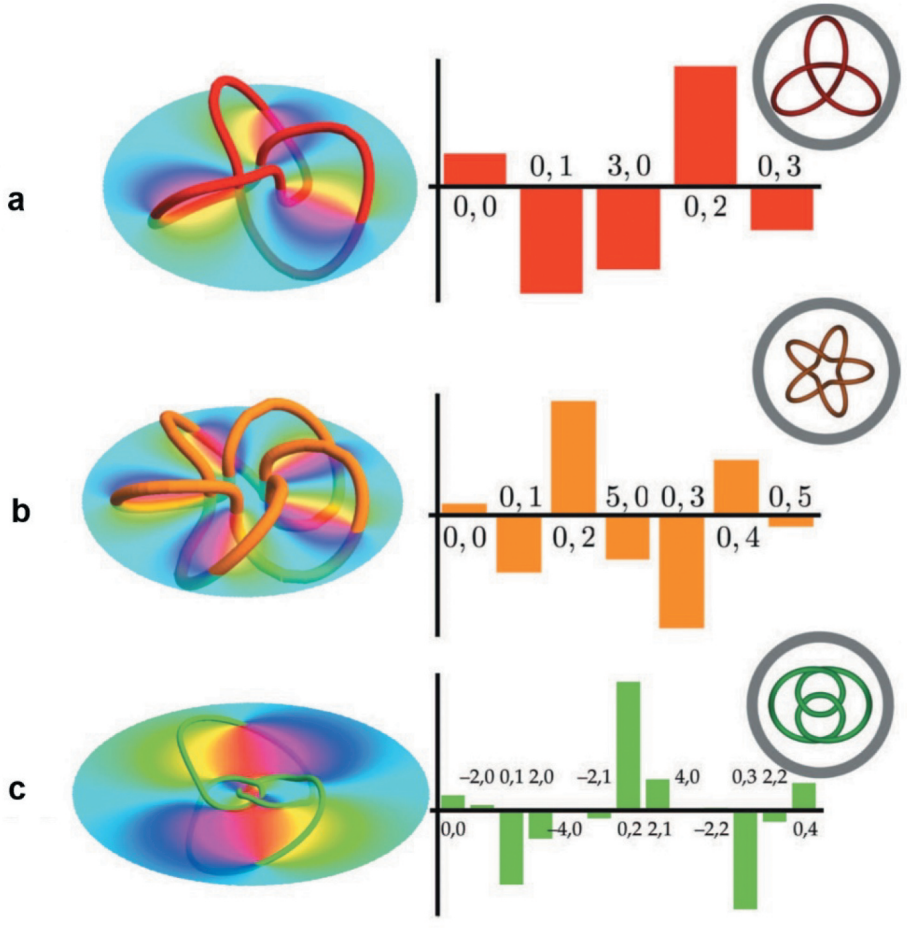

Figure 6. Optical vortex knots constructed from polynomial beams with optimized coefficients [45]. (a) Trefoil. (b) Cinquefoil. (c) Figure-8. Left: vortex line configurations in 3D space and phase distributions at the $z = 0$ plane. Right: the weightings of LG (l, p) components in polynomial. Insets: top view of topologies. Figures reproduced from Ref [45]., copyright 2011, Taylor & Francis.

singularities in high-dimensional spaces, was introduced to mathematically realize these vortex knots and links [48,66]. As such, a periodic braid enclosed in a cylinder was smoothly mapped onto the solid torus under the Milnor mapping that the top and bottom of the cylinder bent around to meet each other, as schematically shown in Figures 5(a) and 5(d), so that the braided vortex line was spliced into an isolated loop residing on a torus, e.g. torus knot, with the height coordinate h replaced by the torus azimuth. This typical configuration is defined by two coprime integer numbers (n,m) in such a way the vortex line winds n times around a circle inside the torus and m times around a line through the hole in the torus [34]. Figures 5(b) and 5(e) plot the corresponding trefoil and figure-8 knots, whose phase distributions at the $z = 0$ plane are shown in Figures 5(c) and 5(f) [48].

In this kind of modal superpositions, the topological behavior of the vortex lines can be predicted with polynomial beams. Yet the linked vortex lines intertwine within regions of very low optical intensity; thus, the reconnection is extremely sensitive to perturbations in the constituent beams. In order to realize the polynomial beams physically, in practice, they are replaced by the realizable beams that satisfy the optical wave equation, e.g. such as LG beams, so that the vortex knot within superposition field has a finite scale. Moreover, these LG components should have a same Gaussian background [48]. Consequently, the z-dependent Gouy phase shift of these LG components induces variant vortex to construct knots in a confined space [67]. Therefore, the practical generation of these topological features with robust topology relies on the numerical optimization of the complex mode coefficients and the size of Gaussian background. Figure 6 shows some vortex knots constructed by polynomial beams with optimized complex coefficients [45].

In the linear homogeneous media, the diffraction and dispersion may diffuse the field structure and reduce the interference contrast. For instance, under the effect of a diffractive background, the vortex and knot corresponding to the destructive dark line are non-separable after a certain diffraction distance. To overcome this issue, Veretenov studied a new class of 3D topological dissipative solitons in homogeneous laser media with fast saturable absorption, namely, hula-hoop solitons [68], which combined the topological structures like vortex knots and the stability of solitons, supplying the potentials of optical information processing, including coding of topologically stable 3D symbols.

Besides, there also are exotic time-dependent solutions of Maxwell's equations, whose electric and magnetic field lines preserve topological configurations [34,41,69,70]. For example, Irvine and Bouwmeester studied the exact knotted solutions in free space based on a topological construction known as a Hopf fibration, in which all electric and magnetic field lines were closed loops and any two electric or magnetic field lines encode into knots

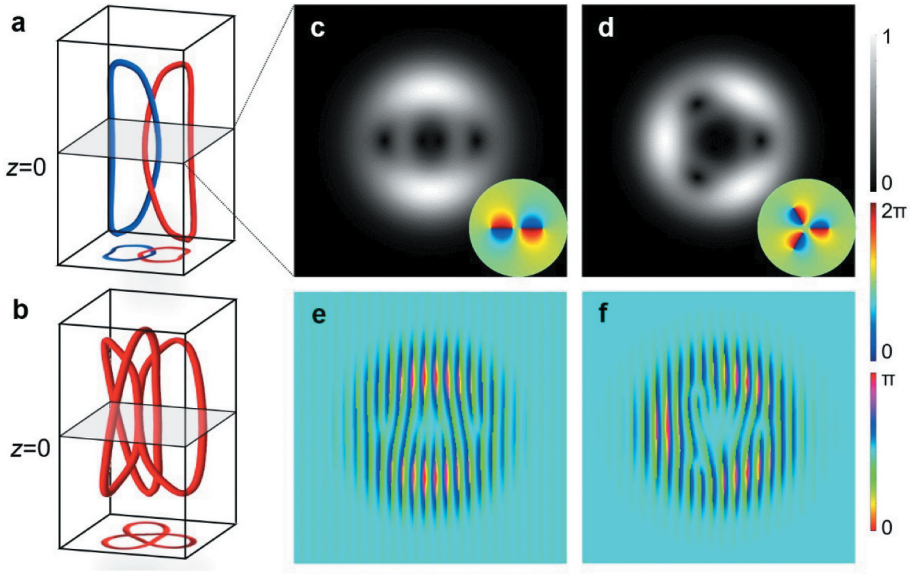

Figure 7. (a), (b) 3D views of isolated Hopf link and trefoil knot [73]. (c), (d) Amplitude and phase (insets) distributions of the Hopf linked and trefoil knotted fields at the waist plane. (e), (f) Phase-only holograms generated by the inverse sinc functional phase-only encoding technique corresponding to the Hopf linked and trefoil knotted fields. Figures reproduced from ref [73]., copyright 2020, Chinese physical society and IOP Publishing Ltd.

and links [47]. Importantly, although these electric and magnetic fields expanded and deformed along with time, their topologies were preserved, as the helicity of the field configuration kept a conserved quantity.

5. SLM realizations

Owing to the requirement of exact control on the complex coefficients of vortex carrying and perturbed components, holography is the most convenient and accurate approach [71]. To implement the hologram design, a programmable spatial light modulator (SLM) is the common device [72]. Such device is composed of liquid crystal arrays, which introduce spatially dependent phase retardation or amplitude modulation across the beam profile, by uploading calculated gray patterns. Compared with a static hologram, the SLM allows controlling the beam parameters dynamically. However, limited by the response freedom of degree of wavefront parameter, e.g. most of the commercial SLM products are of phase-only type, it is necessary to design a phase-only hologram, which can control not only the phase structure of the diffracted beam but also its intensity [46].

In the experiment, the holograms uploaded into the SLM are calculated from the complex amplitude distributions of the knotted or linked fields in their waist plane. The SLM regenerates appropriate interference patterns,

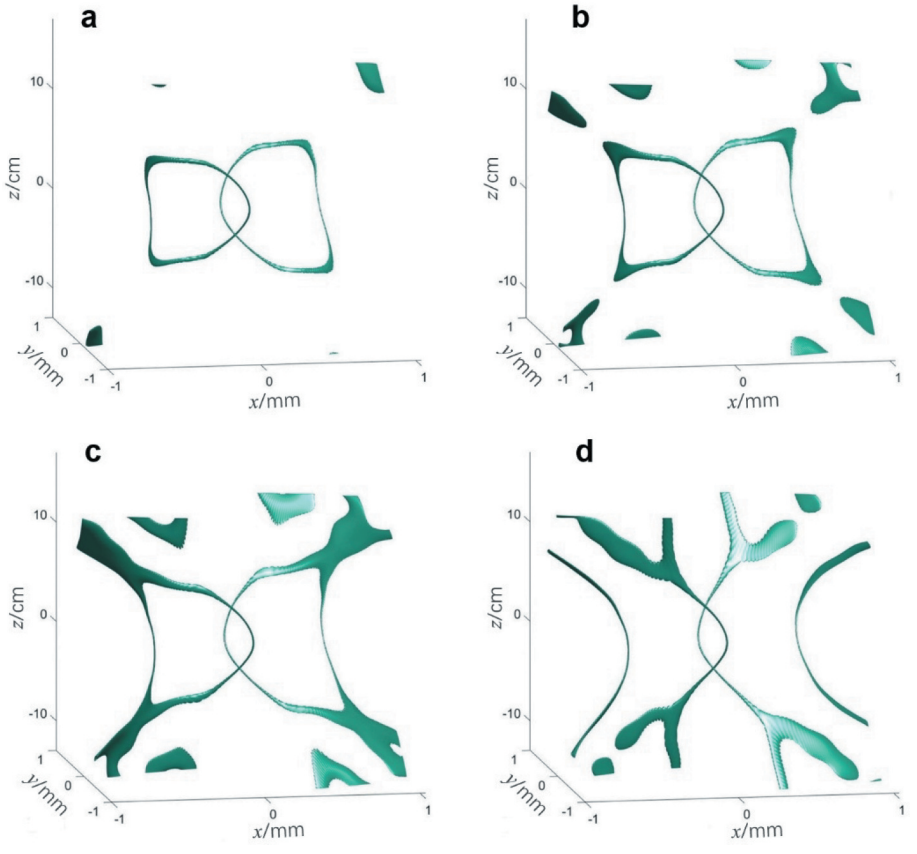

Figure 8. Variation of 3D vortex lines with the decrease of the waist w_0 of the incident Gaussian beam [73]. (a) $w_0 \to \infty$; (b) $w_0 = 8$; (c) $w_0 = 6$; (d) $w_0 = 4$. The vortex lines are mapped from the connection of phase singularities. w_0 is a normalized waist with respect to the pre-modulated w. Figures reproduced from ref [73]., Copyright 2020, Chinese physical society and IOP publishing Ltd.

pixel by pixel, and the desired topologies will be reconstructed within light fields nearby the output plane of a 4 f system [46]. For example, Figures 7(a) and 7(b) illustrate the construction of a Hopf link and trefoil knot based on the LG polynomial beams with a finite width [73]. Suppose that these LG components are modulated by a perturbation term and Gaussian background, the knotted and linked fields at the $z = 0$ plane thus can be described as $\psi_{\text{link, knot}} = \Sigma a_i \text{LG}(l,p,w_0)$, with a_i the coefficient of LG field, and w_0 the waist width that determines the 3D scale of isolated topology, and the corresponding amplitude and phase distributions are shown in Figures 7(c) and 7(d), respectively. Figures 7(e) and 7(f) show the corresponding phase-only holograms via the inverse sinc function encoding method. Besides SLM, efficient optical devices with smaller pixel, e.g. geometric phase liquid crystal plate, have been used to create optical vortex knots and links [73].

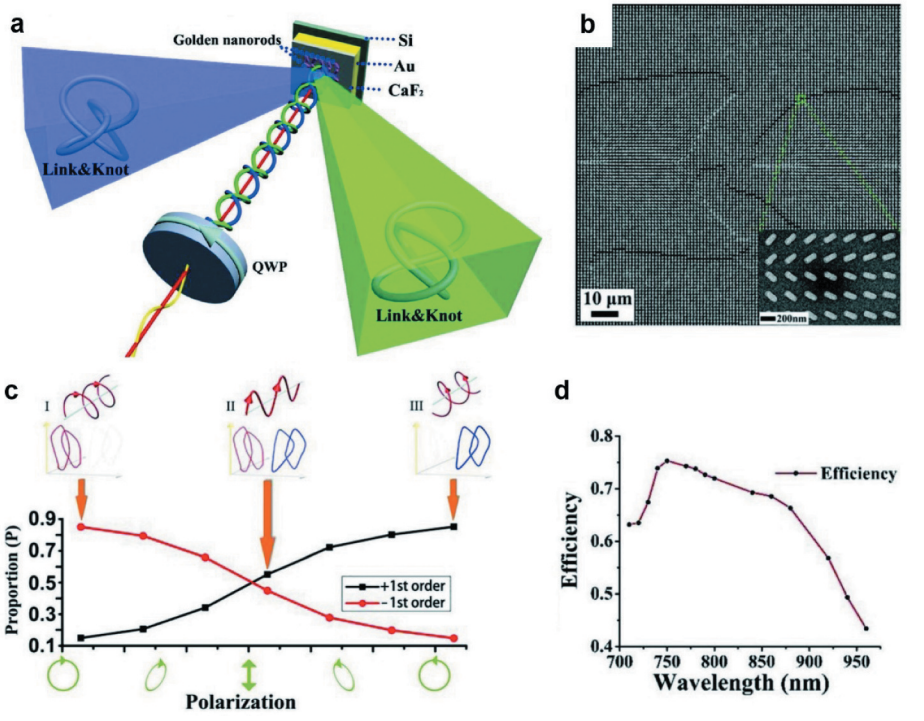

Figure 9. A metal metasurface to generate ultrasmall vortex knot and link [87]. (a) Schematic of construction principle. (b) SEM image of Hopf link metasurface. (c) Result (Hopf link) with the incident light changing from the left circular polarization to right circular polarization. (d) Experimentally obtained optical efficiencies of a trefoil knot. Figures reproduced from ref [87]., copyright 2019, WILEY-VCH.

It is noteworthy that the size of the Gaussian background in polynomial beams significantly affects the topological configuration [48]. For the holographic method, the incident beam size can likewise affect the topological structure. Figure 8 displays the numerically configured Hopf links under the illuminations of Gaussian beams with different waists [73]. As shown in Figure 8(a), for a plane wave incidence, an isolated vortex link occurs because of the pre-modulated waist in the hologram. As the decrease of the waist radius, extra vortex lines appear and go close to the isolated vortex link. Once the incident beam waist is small enough, extra vortex lines reconnect with the isolated vortex lines, and then the isolated topological link is broken. This also proves that the holographic method guarantees sufficient generation robustness.

For the common generation approach based on holography, the reconstruction quality is closely dependent on the response of device pixel. For the SLM, relatively large pixel size induces the disadvantages such as misalignment and pixelation, which limit the construction perfection.

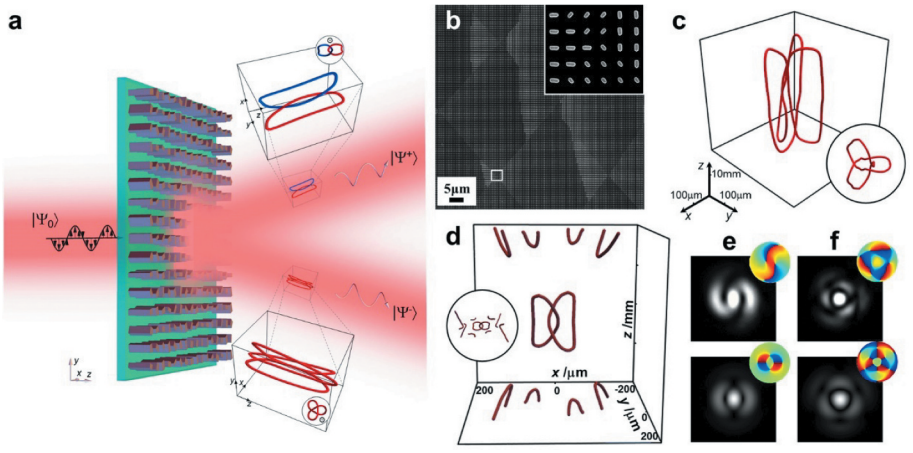

Figure 10. Tying polarization-switchable vortex knot and link via a dielectric metasurface [88]. (a) Schematic of tying polarization-switchable knot and link. (b) SEM image of metasurface for tying trefoil knot. (c) Detected trefoil knot configuration. (d) Vortex lines structure beyond the isolated Hopf link. (e), (f) Intensity and phase distributions of field obtained from the far-field detection and the Fourier transform of field at the $z = 0$ plane, respectively. Left: Hopf link; right: trefoil knot. Figures reproduced from ref [88]., copyright 2020, WILEY-VCH.

Therefore, efficient optical device with smaller pixel is necessary to overcome such issues.

6. Metasurface realizations

Anisotropic metasurfaces, which work as nanoscale birefringent phase-shifters, in recent years have been substantially studied [74], showing application prospects in achromatic metalens [75], polarization-dependent holographic display [76], broadband response [77], and efficient optical devices [78] et al. This artificially planar material enables the simultaneous modulation of local phase, amplitude, and polarization of light field in subwavelength scale, molds optical wavefront into arbitrary mode, providing a new possibility for the miniaturization and integration of modern optical devices [79–83]. Typically, various metasurfaces have been proposed with advantages in applications associated with optical vortex, such as OAM holography [84], multiplexing, and demultiplexing [85] et al.

Compared with conventional technologies referring to SLMs, holography based on metasurfaces exhibits significant advantages in the control of polarization and large view angle [86], because of their inherent properties of ultra-small pixel, polarization response, and flexible phase gradient. More recently, some subtle metasurfaces have been proposed to the construction of topological optical fields with ultrasmall scale [87–90]. Typically, a metal type metasurface that consists of rectangular gold nanorods was proposed to realize the holographic reconstruction of vortex knots and links [87]. This

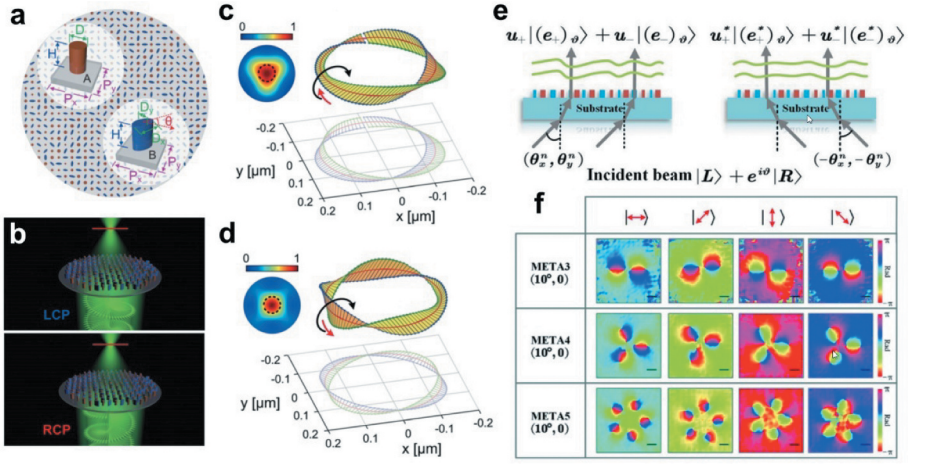

Figure 11. 3D optical polarization topologies enabled by all-dielectric metasurfaces. (a) Schematic diagram of all-dielectric metasurface for the construction of spin-controlled Möbius strip [100]. (b)-(d) Retrieved polarization topological configurations at the focal plane, when LCP and RCP light illuminate the metasurface. (e) Schematic illustration of the coherent pixel polarization metaholography [89]. (f) Experimental results of the Hopf link, trefoil and cinquefoil polarization knot profiles with different linearly polarized light illuminations. Figures reproduced from: (a)-(d) ref [100]., copyright 2019, The Royal Society of Chemistry; (e)-(f) ref [89]., copyright 2020, WILEY-VCH.

reflective metal metasurface was designed based on the Pancharatnam-Berry (PB) phase, according to the pure phase-encoded holograms calculated from the complex amplitude of the Hopf linked or trefoil knotted light field at the $z = 0$ plane. The schematic of tying ultrasmall vortex knot and link is shown in Figure 9(a).

When a circularly polarized light was incident vertically, it produced topological knot or link that was six orders of magnitude smaller than the SLM method. Remarkably, due to the spin–orbit interaction, the angular position of the reconstructed topology was dependent on the incident circular polarization state [see Figure 9(c)]. Moreover, because of the PB phase modulation mechanism, this kind of metasurface had the advantage of broadband response at the NIR frequency with high efficiency, as shown in Figure 9(d).

A holographic all-dielectric metasurface based on the combination of PB phase and propagation phase was proposed, to compact and reconstruct multichannel topological configurations [88]. The knotted and linked fields at the $z = 0$ plane were decomposed into LG polynomial components, as a slice of a Milnor polynomial. Such two typical fields were encoded into respective holograms via the inverse sinc functional phase-only encoding technique, and then these two holograms were combined onto the dielectric metasurface composed of rectangle pillars with variant

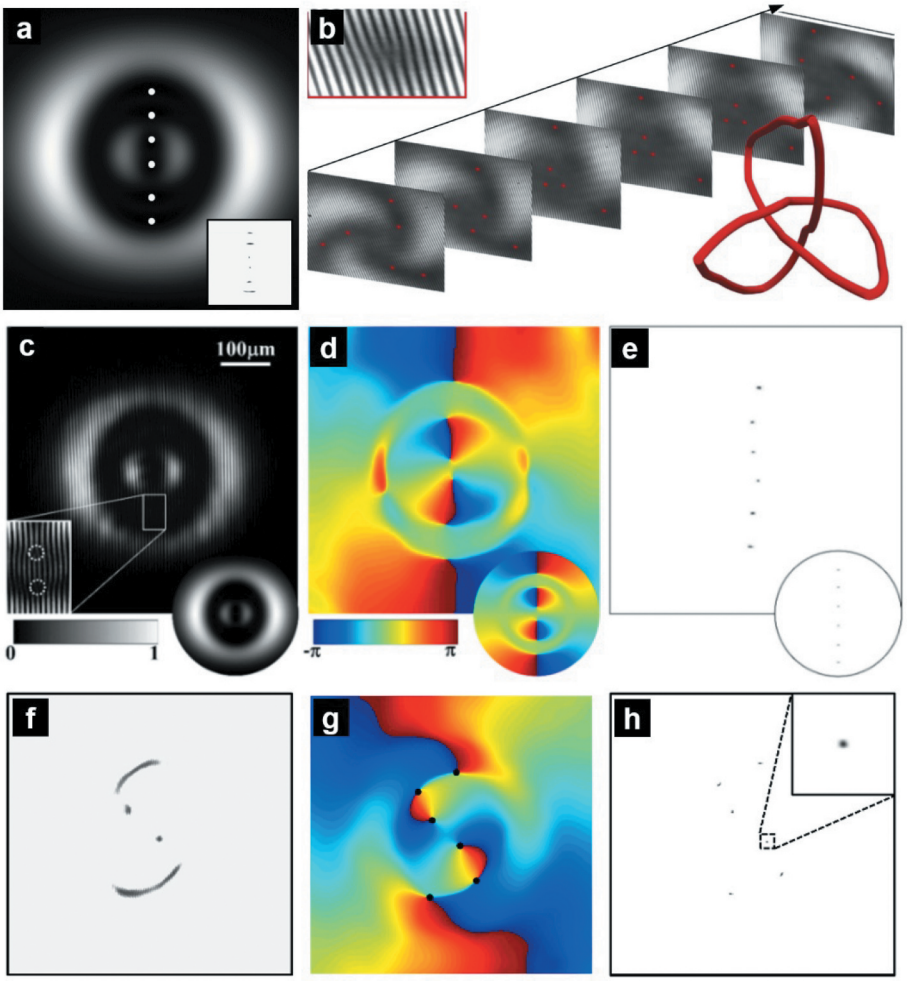

Figure 12. Experiment results of a vortex link. (a) Intensity distribution of field at the waist plane. These white points depict the vortex singularities. Inset: overexposure intensity pattern. (b) Locating method via interference [72]. (c) Holographic interferogram [103]. (d) Corresponding phase distribution reconstructed by digital holography. (e) Singularity positions located from phase pattern. Insets: the corresponding theoretical results shown in the bottom. (f) Overexposure intensity distribution of vortex field in the plane near to inflexion of vortex lines. (g) Demodulated phase from hologram; (h) Singularity map calculated by the phase singularity locating algorithm. Figures reproduced from: (b) ref [72]., Copyright 2016, nature publishing group; (c) – (h) ref [103]., copyright 2020, optical society of America.

geometry and orientation angle, based on the independent spin modulation mechanism.

As Figure 10(a) shows, for the incidence of a linearly polarized beam, polarization-switchable topological configuration with ultras-mall size, e.g. trefoil knot and Hopf link, were configured. Likewise, by using the phase singularity locating method, as to be described in Section 7, such small

topologies were also accurately mapped and analyzed. An experimental map trefoil knot is shown in Figure 10(c). Importantly, although the topological configuration occupied a finite volume of space, as the isolated link shown in Figure 10(d), this topology affected the entire wavefield, even the far-field structure. Figures 10(e) and 10(f) compare the intensity and phase distributions of field beyond the isolated link and knot, which are obtained from the far-field detection and the Fourier transform of field at the $z = 0$ plane, respectively. These ultra-small topological fields and the vortex structures show robust configuration conservation property.

For the optical vortex knots and links generated from holographic metasurface, the configuration scale is determined by the metasurface dimension. In other words, the advantage of metasurface in dimension enables the possibility of further decreasing the magnitude of topological configuration. As the theory predicts, the topological structure can be modulated further to the scale of several wavelengths by adjusting the fabrication device, on the premise that the integrity of the phase profile can be reconstructed. For instance, the acoustic vortex knots were recently realized via holographic metamaterials with only 24×24 pixels [90]. The measured Hopf link and trefoil knot configurations have been reduced to about 4λ transversely, and about 8λ longitudinally, at wavelength scale.

The research on the polarization singularity has long history likewise the phase singularity, because of the crucial role of polarization response in light–matter interaction. In the past decade, the vector beams embedded with on-axis polarization singularities [91], namely, polarization vortices, whose polarization azimuths are undefined, akin to the first type vortex beam, have attracted tremendous interests, because of their unique advantages for the construction of light fields that break the diffraction limitation and present delicate spatial and polarization structures [92–96]. Furthermore, some typical topological structures, e.g. polarization Möbius strip [97], have been constructed by the tightly focusing of vector fields. Recently, 3D polarization knots composed by vortex singularities of complex Stokes field $s_1 + is_2$, such as the torus knots and links as well as the complicated figure-8 knot, have been generated based on the superposition of a traditional knotted vortex beam and a Gaussian beam with opposite spin states [98,99].

As the advantages of more degrees of freedom and miniaturization, the knot and link with controllable topological configurations formed by the polarization singularity have been achieved with the help of metasurfaces. Figure 11(a) shows an ultrathin all-dielectric metasurface that can achieve efficient generation and transformation of two arbitrary 3D polarization topologies [100]. This metasurface consists of two distinct elements, which are designed for the generation of tightly focused Poincaré beams composed of Gauss and LG components with opposite spin states. For the illuminations of the LCP or RCP light beams, it produces a Möbius strip

with three or four half-twists. Similarly, a composite metasurface that enables complete control of arbitrary spatially varying polarization fields has been proposed to generate polarization knots [89]. This metasurface was designed according to a coherent pixel polarization metahologram, which can be used to generate angle-multiplexed output fields with orthogonal polarization pairs to construct polarization knots. As shown in Figure 11(f), three azimuth-controllable polarization knot profiles where the C-points of the polarization singularities are unchanged were experimentally realized.

7. Characterizing topological configurations

Several methods have been proposed to observe the vortex topologies, of which the key point is how to locate the phase singularity accurately. The most widely used method is detecting the locations of dark cores caused by singularities [31,46], that is, intensity locating method. For this kind of method, consider that the fine details of the vortex lines lie in regions of near darkness and in order to measure the vortex positions within the beam cross-section directly, it is necessary to over-saturate the record CCD. Figure 12(a) illustrates the experimental results of the intensity distributions of a link threaded by two vortex lines at the $z = 0$ plane, where the inset shows the overexposure intensity pattern. As shown, the resulted image is mainly white, but contains points of darkness corresponding to the vortices as they intersected the plane of the CCD. After the z-scanning detection, the combination of transverse vortex coordinates measured in neighbouring planes enables the configuration of 3D topological structures. This overexposure intensity method has a rapid speed to locate the singularities. However, the locating accuracy is unsatisfactory, in an ultra-small topological light field, because the dark spots are not so small enough when the background field is weak, and then several singularities that close together overlap, as the results shown in Figure 12(h).

One improved method that locates the positions of phase singularities from the forked stripe within interferogram produced by the vortex field and a reference planar wave was proposed [72], as shown in Figure 12(b). The locating precision of this method is mainly limited by the period of interference fringes. Further, a method based on phase pattern has been proposed, where the singularities are located from considering the phase change around a small loop of pixels [101]. Likewise, this method is inaccurate for the case of multiple singularities coexisting in an ultra-small topological light field. To measure the phase distribution of the entire optical field, the phase shift method is necessary [102], which requires a multi-step measurement of each plane, greatly decreasing the measuring speed and increasing the reconstruction error.

Recently, a more accurate and rapid method to experimentally map the topology configuration of optical vortex has been reported [103], in which the phase distribution in any transverse plane was firstly measured by the digital holography, and the location of phase singularity was accurately obtained by utilizing a numerical search algorithm based on local spatial frequency. Meanwhile, self-calibration property between multi-plane singularities was adopted for 3D reconstruction of vortex lines. Figures 12(d-f) shows the locating process of phase singularities based on the digital holography. In contrast to the overexposure intensity method, this method has higher precision in locating the inflexion of vortex lines, as the experiment results shown in Figures 12(g-i).

8. Applications

The light embedded with optical vortex has OAM and associated transverse energy flow and thus can exert a torque, which has been widely exploited in particle manipulations as light spanners [104,105]. Knotted optical fields supply the possibility of extended and knotted optical manipulations in three dimensions. This hypothesis was recently realized by light fields with knotted trajectories of bright spots [106], whose intensities are complementary to the knotted vortex lines, with multi-particle transport in knot circuits and networks under programmable paths [107].

Knot theory has already influenced particular areas of physics, e.g. topological quantum computing, where knot can be used as 'quantum core'. Entanglement of linked optical vortex loops in the light, within macroscopic and finite volumes, was realized by spontaneous parametric down-conversion [108]. This entanglement of photons in complex 3D topological states suggests the possibility of entanglement of similar features in other systems. In addition, the knotted fields can act as synthetic gauge fields on neutral atomic gas, and transfer the topological properties to the ground state of a 3D Bose–Einstein condensate [65].

9. Conclusion and outlook

With the deepening of research on light field modulation, novel light fields with distinct configurations have been continuously developed, which sufficiently support for expanding the application of structured light fields. As above mentioned, in order to make the polynomial beams physically realizable, the polynomial is multiplied by a Gaussian amplitude function with width. Therefore, the size of the topology is order of the waist radius transversely (10^3–$10^4\lambda$), but of the Rayleigh length longitudinally (10^6–$10^8\lambda$) [109]. This extreme aspect ratio is impractical to imprint into material systems, such as ferroelectrics [110] and chiral nematic colloids [111]. Fortunately, with the

development of sub-wavelength and near-field wavefront control technologies such as metasurfaces, and nonparaxial modulation methods such as tightly focusing, the configuration dimension can be further decreased.

Once the topological configuration is compressed to the wavelength scale and even smaller, the imprint possibility between it and the material structure will greatly promote the development of light–matter interaction. Remarkably, this ultra-small-structured light field provides the possibility to construct knotted structures in photosensitive materials, and even to control the velocity of a vortex knot excited in the superfluid wave function of a Bose–Einstein condensate [63].

As topologically stable objects in field theories, knots have been put forward to explain various persistent phenomena in systems ranging from atoms and molecules to cosmic textures in the universe. The topological manipulation observed in other wave system [112], such as the tying and untying knots that occur in hydrodynamics [113], can be realized in optical system, utilizing the holographic reconstruction method based on polynomial beams. Topology switch and even the continuous transformation will bring new opportunities for topological information processing.

Disclosure statement

No potential conflict of interest was reported by the authors.

Funding

This work was supported by the National Key Research and Development Program of China (2017YFA0303800), National Natural Science Foundation of China (NSFC) (11634010, 91850118, 11774289, 61675168, 11804277), Natural Science Basic Research Program of Shaanxi (2020JM-104), Fundamental Research Funds for the Central Universities (3102018zy036, 3102019JC008, 310201911cx022), Innovation Foundation for Doctor Dissertation of Northwestern Polytechnical University (CX202046, CX202048);National Natural Science Foundation of China [11634010, 91850118, 11774289, 61675168, 11804277];Natural Science Basic Research Program of Shaanxi [2020JM-104];Innovation Foundation for Doctor Dissertation of Northwestern Polytechnical University [CX202046, CX202048];Fundamental Research Funds for the Central Universities [3102018zy036, 3102019JC008, 310201911cx022];National Key Research and Development Program of China [2017YFA0303800];

References

[1] Rubinsztein-Dunlop H, Forbes A, Berry MV, et al. Roadmap on structured light. J Opt. 2017;19:51.
[2] Soskin MS, Vasnetsov MV. Singular optics. Prog Opt.. 2001;42:219–276.
[3] Dennis MR, O'Holleran K, Padgett MJ. Optical vortices and polarization singularities. Prog Opt. 2009;53:293–363.

[4] Visser TD. Detecting the colours of darkness. Phys World. 2004;17:20.
[5] Owczarek R, Slupski T. Quantum vortex waves in superfluid helium: A Hamiltonian approach. Physica B. 1992;182:278–286.
[6] Blatter G, Feigel'man MV, Geshkenbein VB, et al. Vortices in high-temperature superconductors. Rev Mod Phys. 1994;66:1125–1388.
[7] Bewley GP, Lathrop DP, Sreenivasan KR. Visualization of quantized vortices. Nature. 2006;441:588.
[8] Lagoudakis KG, Wouters M, Richard M, et al. Quantized vortices in an exciton–polariton condensate. Nat Phys. 2008;4:706–710.
[9] Nagaosa N, Tokura Y. Topological properties and dynamics of magnetic skyrmions. Nat Nanotechnol. 2013;8:899–911.
[10] Ozawa T, Price HM, Amo A, et al. Topological photonics. Rev Mod Phys. 2019;91:015006.
[11] Song D, Leykam D, Su J, et al. Valley vortex states and degeneracy lifting via photonic higher-band excitation. Phys Rev Lett. 2019;122:123903.
[12] Song D, Paltoglou V, Liu S, et al. Unveiling pseudospin and angular momentum in photonic graphene. Nat Commun. 2015;6:6272.
[13] Dominici L, Carretero-González R, Gianfrate A, et al. Interactions and scattering of quantum vortices in a polariton fluid. Nat Commun. 2018;9:1467.
[14] Bewley GP, Paoletti MS, Sreenivasan KR, et al. Characterization of reconnecting vortices in superfluid helium. Proc Natl Acad Sci USA. 2008;105:13707–13710.
[15] Moffatt HK. Helicity and singular structures in fluid dynamics. Proc Natl Acad Sci USA. 2014;111:3663–3670.
[16] Wang Z, Chong Y, Joannopoulos JD, et al. Observation of unidirectional backscattering-immune topological electromagnetic states. Nature. 2009;461:772–775.
[17] Tewari S, Das Sarma S, Nayak C, et al. Quantum computation using vortices and majorana zero modes of a p_x+ip_y superfluid of fermionic cold atoms. Phys Rev Lett. 2007;98:010506.
[18] Cardano F, D'Errico A, Dauphin A, et al. Detection of Zak phases and topological invariants in a chiral quantum walk of twisted photons. Nat Commun. 2017;8:15516.
[19] Nye JF, Berry MV, Frank FC. Dislocations in wave trains. P Roy Soc Lond A-Math Phys Sci. 1974;336:165–190.
[20] Coullet P, Gil L, Rocca F. Optical vortices. Opt Commun. 1989;73:403–408.
[21] Allen L, Beijersbergen MW, Spreeuw RJC, et al. Orbital angular momentum of light and the transformation of Laguerre-Gaussian laser modes. Phys Rev A. 1992;45:8185–8189.
[22] Molina-Terriza G, Torres JP, Torner L. Twisted photons. Nat Phys. 2007;3:305–310.
[23] Franke-Arnold S, Allen L, Padgett M. Advances in optical angular momentum. Laser Photonics Rev. 2008;2:299–313.
[24] Grier DG. A revolution in optical manipulation. Nature. 2003;424:810–816.
[25] Bozinovic N, Yue Y, Ren Y, et al. Terabit-scale orbital angular momentum mode division multiplexing in fibers. Science. 2013;340:1545–1548.
[26] Yao AM, Padgett MJ. Orbital angular momentum: origins, behavior and applications. Adv Opt Photon. 2011;3:161–204.
[27] Faddeev L, Niemi AJ. Stable knot-like structures in classical field theory. Nature. 1997;387:58–61.
[28] Battye RA, Sutcliffe PM. Knots as stable soliton solutions in a three-dimensional classical field theory. Phys Rev Lett. 1998;81:4798–4801.

[29] Samuels DC, Barenghi CF, Ricca RL. Quantized vortex knots. J Low Temp Phys. 1998;110:509–514.
[30] Hietarinta J, Salo P. Faddeev-Hopf knots: dynamics of linked un-knots. Phys Lett B. 1999;451:60–67.
[31] Leach J, Dennis MR, Courtial J, et al. Knotted threads of darkness. Nature. 2004;432:165.
[32] Kawaguchi Y, Nitta M, Ueda M. Knots in a spinor bose-einstein condensate. Phys Rev Lett. 2008;100:180403.
[33] Scheeler MW, Kleckner D, Proment D, et al. Helicity conservation by flow across scales in reconnecting vortex links and knots. Proc Natl Acad Sci USA. 2014;111:15350–15355.
[34] Arrayas M, Bouwmeester D, Trueba JL. Knots in electromagnetism. Phys Rep. 2017;667:1–61.
[35] Martinez A, Ravnik M, Lucero B, et al. Mutually tangled colloidal knots and induced defect loops in nematic fields. Nat Mater. 2014;13:258–263.
[36] Klembt S, Harder TH, Egorov OA, et al. Exciton-polariton topological insulator. Nature. 2018;562:552–556.
[37] Sato M, Ando Y. Topological superconductors: a review. Rep Prog Phys. 2017;80:076501.
[38] Rechtsman MC, Zeuner JM, Plotnik Y, et al. Photonic Floquet topological insulators. Nature. 2013;496:196–200.
[39] Hall DS, Ray MW, Tiurev K, et al. Tying quantum knots. Nat Phys. 2016;12:478–483.
[40] Duan Y-S, Zhao L, Zhang X-H. Topological structure of knotted vortex lines in liquid crystals. Commun Theor Phys. 2007;47:1129–1134.
[41] Kedia H, Bialynicki-Birula I, Peralta-Salas D, et al. Tying knots in light fields. Phys Rev Lett. 2013;111:5.
[42] Kleckner D, Irvine WTM. Creation and dynamics of knotted vortices. Nat Phys. 2013;9:253–258.
[43] Adams CS, Riis E. Laser cooling and trapping of neutral atoms. Prog Quant Electron. 1997;21:1–79.
[44] Wang J. Advances in communications using optical vortices. Photon Res. 2016;4: B14–B28.
[45] Padgett MJ, O'Holleran K, King RP, et al. Knotted and tangled threads of darkness in light beams. Contemp Phys. 2011;52:265–279.
[46] Leach J, Dennis MR, Courtial J, et al. Vortex knots in light. New J Phys. 2005;7:11.
[47] Irvine WTM, Bouwmeester D. Linked and knotted beams of light. Nat Phys. 2008;4:716–720.
[48] Dennis MR, King RP, Jack B, et al. Isolated optical vortex knots. Nat Phys. 2010;6:118–121.
[49] Vaughan JM, Willetts DV. Interference properties of a light beam having a helical wave surface. Opt Commun. 1979;30:263–267.
[50] O'Holleran K, Dennis MR, Padgett MJ. Topology of light's darkness. Phys Rev Lett. 2009;102:4.
[51] Berry MV, Dennis MR. Knotted and linked phase singularities in monochromatic waves. Proc R Soc.A-Math Phys Eng Sci. 2001;457:2251–2263.
[52] O'Holleran K, Dennis MR, Flossmann F, et al. Fractality of light's darkness. Phys Rev Lett. 2008;100:4.
[53] O'Neil AT, MacVicar I, Allen L, et al. Intrinsic and Extrinsic Nature of the Orbital Angular Momentum of a Light Beam. Phys Rev Lett. 2002;88:053601.

[54] Orlov S, Regelskis K, Smilgevičius V, et al. Propagation of Bessel beams carrying optical vortices. Opt Commun. 2002;209:155–165.
[55] Biener G, Gorodetski Y, Niv A, et al. Manipulation of polarization-dependent multi-vortices with quasi-periodic subwavelength structures. Opt Lett. 2006;31:1594–1596.
[56] Bliokh K, Rodríguez-Fortuño F, Nori F, et al. Spin-orbit interactions of light. Nat Photonics. 2015;9:796–808.
[57] Li P, Liu S, Zhang Y, et al. Modulation of orbital angular momentum on the propagation dynamics of light fields. Frontiers of Optoelectronics. 2019;12:69–87.
[58] Zhang Y, Li P, Liu S, et al. Unveiling the photonic spin Hall effect of freely propagating fan-shaped cylindrical vector vortex beams. Opt Lett. 2015;40:4444–4447.
[59] Lloyd SM, Babiker M, Thirunavukkarasu G, et al. Electron vortices: beams with orbital angular momentum. Rev Mod Phys. 2017;89:035004.
[60] Hong Z, Zhang J, Drinkwater BW. Observation of orbital angular momentum transfer from Bessel-shaped acoustic vortices to diphasic liquid-microparticle mixtures. Phys Rev Lett. 2015;114:214301.
[61] Shen Y, Wang X, Xie Z, et al. Optical vortices 30 years on: OAM manipulation from topological charge to multiple singularities. Light Sci Appl. 2019;8:1–29.
[62] O'Holleran K, Padgett MJ, Dennis MR. Topology of optical vortex lines formed by the interference of three, four, and five plane waves. Opt Express. 2006;14:3039–3044.
[63] Proment D, Onorato M, Barenghi CF. Vortex knots in a Bose-Einstein condensate. Phys Rev E. 2012;85:8.
[64] Salman H. Helicity conservation and twisted Seifert surfaces for superfluid vortices. Proc R Soc A-Math Phys Eng Sci. 2017;473:20160853.
[65] Duncan CW, Ross C, Westerberg N, et al. Linked and knotted synthetic magnetic fields. Phys Rev A. 2019;99:7.
[66] Bode B, Dennis MR, Foster D, et al. Knotted fields and explicit fibrations for lemniscate knots. Proc R Soc A-Math Phys Eng Sci. 2017;473:20160829.
[67] Baumann SM, Kalb DM, MacMillan LH, et al. Propagation dynamics of optical vortices due to Gouy phase. Opt Express. 2009;17:9818–9827.
[68] Veretenov NA, Fedorov SV, Rosanov NN. Topological vortex and knotted dissipative optical 3D solitons generated by 2D vortex solitons. Phys Rev Lett. 2017;119:5.
[69] de Klerk A, van der Veen RI, Dalhuisen JW, et al. Knotted optical vortices in exact solutions to Maxwell's equations. Phys Rev A. 2017;95:5.
[70] Valverde AM, Angulo LD, Cabello MR, et al. Numerical simulation of knotted solutions for Maxwell equations. Phys Rev E. 2020;101:6.
[71] Wilson M. Holograms tie optical vortices in knots. Phys Today. 2010;63:18–20.
[72] Tempone-Wiltshire SJ, Johnstone SP, Helmerson K. Optical vortex knots - one photon at a time. Sci Rep. 2016;6:6.
[73] Guo X, Zhong J, Li P, et al. Creation of topological vortices using Pancharatnam-Berry phase liquid crystal holographic plates. Chin Phys B. 2020;29:040305.
[74] Yu N, Capasso F. Flat optics with designer metasurfaces. Nat Mater. 2014;13:139–150.
[75] Wang S, Wu PC, Su V-C, et al. Broadband achromatic optical metasurface devices. Nat Commun. 2017;8:187.
[76] Wen D, Yue F, Li G, et al. Helicity multiplexed broadband metasurface holograms. Nat Commun. 2015;6:8241.
[77] Chen WT, Zhu AY, Sanjeev V, et al. A broadband achromatic metalens for focusing and imaging in the visible. Nat Nanotechnol. 2018;13:220–226.
[78] Zheng G, Mühlenbernd H, Kenney M, et al. Metasurface holograms reaching 80% efficiency. Nat Nanotechnol. 2015;10:308–312.

[79] Zhang L, Mei S, Huang K, et al. Advances in full control of electromagnetic waves with metasurfaces. Adv Opt Mater. 2016;4:818–833.
[80] Liu W, Li Z, Li Z, et al. Energy-tailorable spin-selective multifunctional metasurfaces with full Fourier components. Adv Mater. 2019;31:1901729.
[81] Chen S, Liu W, Li Z, et al. Metasurface-empowered optical multiplexing and multifunction. Adv Mater. 2020;32:2070022.
[82] Liu W, Cheng H, Tian J, et al. Diffractive metalens: from fundamentals, practical applications to current trends. Adv Phys X. 2020;5:1742584.
[83] Fan X, Li P, Guo X, et al. Axially tailored light field by means of a dielectric metalens. Phys Rev Appl. 2020;14:024035.
[84] Ren H, Briere G, Fang X, et al. Metasurface orbital angular momentum holography. Nat Commun. 2019;10:1–8.
[85] Li Y, Li X, Chen L, et al. Orbital angular momentum multiplexing and demultiplexing by a single metasurface. Adv Opt Mater. 2017;5:1600502.
[86] Deng Z-L, Li G. Metasurface optical holography. Mater Today Phys. 2017;3:16–32.
[87] Wang L, Zhang W, Yin H, et al. Ultrasmall optical vortex knots generated by spin-selective metasurface holograms. Adv Opt Mater. 2019;7:1900263.
[88] Guo X, Li P, Zhong J, et al. Tying polarization-switchable optical vortex knots and links via holographic all-dielectric metasurfaces. Laser Photonics Rev. 2020;14:1900366.
[89] Wang E, Niu J, Liang Y, et al. Complete control of multichannel, angle-multiplexed, and arbitrary spatially varying polarization fields. Adv Opt Mater. 2020;8:1901674.
[90] Zhang H, Zhang W, Liao Y, et al. Creation of acoustic vortex knots. Nat Commun. 2020;11:3956.
[91] Qiwen Z. Cylindrical vector beams: from mathematical concepts to applications. Adv Opt Photon. 2009;1:1–57.
[92] Dorn R, Quabis S, Leuchs G. Sharper focus for a radially polarized light beam. Phys Rev Lett. 2003;91:233901.
[93] Zhao Y, Zhan Q, Zhang Y, et al. Creation of a three-dimensional optical chain for controllable particle delivery. Opt Lett. 2005;30:848–850.
[94] Wang X, Chen J, Li Y, et al. Optical orbital angular momentum from the curl of polarization. Phys Rev Lett. 2010;105:253602.
[95] Wang H, Shi L, Lukyanchuk B, et al. Creation of a needle of longitudinally polarized light in vacuum using binary optics. Nat Photonics. 2008;2:501–505.
[96] Du L, Yang A, Zayats AV, et al. Deep-subwavelength features of photonic skyrmions in a confined electromagnetic field with orbital angular momentum. Nat Phys. 2019;15:650–654.
[97] Bauer T, Banzer P, Karimi E, et al. Observation of optical polarization Möbius strips. Science. 2015;347:964–966.
[98] Larocque H, Sugic D, Mortimer D, et al. Reconstructing the topology of optical polarization knots. Nat Phys. 2018;14:1079–1082.
[99] Pisanty E, Machado GJ, Vicuna-Hernandez V, et al. Knotting fractional-order knots with the polarization state of light. Nat Photonics. 2019;13:569-+.
[100] Huo P, Zhang S, Fan Q, et al. Photonic spin-controlled generation and transformation of 3D optical polarization topologies enabled by all-dielectric metasurfaces. Nanoscale. 2019;11:10646–10654.
[101] Oholleran K, Flossmann F, Dennis MR, et al. Methodology for imaging the 3D structure of singularities in scalar and vector optical fields. J Opt. 2009;11:094020.
[102] Brophy CP. Effect of intensity error correlation on the computed phase of phase-shifting interferometry. J Opt Soc Am A. 1990;7:537–541.

[103] Zhong J, Qi S, Liu S, et al. Accurate and rapid measurement of optical vortex links and knots. Opt Lett. 2019;44:3849–3852.
[104] He H, Friese MEJ, Heckenberg NR, et al. Direct observation of transfer of angular momentum to absorptive particles from a laser beam with a phase singularity. Phys Rev Lett. 1995;75:826–829.
[105] Simpson NB, Dholakia K, Allen L, et al. Mechanical equivalence of spin and orbital angular momentum of light: an optical spanner. Opt Lett. 1997;22:52–54.
[106] Shanblatt ER, Grier DG. Extended and knotted optical traps in three dimensions. Opt Express. 2011;19:5833–5838.
[107] Rodrigo JA, Angulo M, Alieva T. Programmable optical transport of particles in knot circuits and networks. Opt Lett. 2018;43:4244–4247.
[108] Romero J, Leach J, Jack B, et al. Entangled optical vortex links. Phys Rev Lett. 2011;106:4.
[109] Sugic D, Dennis MR. Singular knot bundle in light. J Opt Soc Am A. 2018;35:1987–1999.
[110] Luk'yanchuk I, Tikhonov Y, Razumnaya A, et al. Hopfions emerge in ferroelectrics. Nat Commun. 2020;11:2433.
[111] Tkalec U, Ravnik M, Čopar S, et al. Reconfigurable knots and links in chiral nematic colloids. Science. 2011;333:62–65.
[112] Ricca RL, Samuels DC, Barenghi CF. Evolution of vortex knots. J Fluid Mech. 1999;391:29–44.
[113] Kleckner D, Kauffman LH, Irvine WTM. How superfluid vortex knots untie. Nat Phys. 2016;12:650–655.